The Effect of Temperature and Dot Size on the Spectral Properties of Colloidal InP/ZnS Core–Shell Quantum Dots

Arun Narayanaswamy,[†,§] L. F. Feiner[†] A. Meijerink,[‡] and P. J. van der Zaag[†,*]

[†]Philips Research Laboratories, Prof. Holstlaan 4, 5656 AE Eindhoven, The Netherlands, and [‡]Debye Institute, Physics and Chemistry of Condensed Matter, Utrecht University, P.O. Box 80.000, 3508 TA Utrecht, The Netherlands. [§]Current address: CIBA Inc. (part of BASF) Schwarzwaldalle 215, R-1059.5.14, 4002 Basel, Switzerland.

ABSTRACT Visual color changes between 300 and 510 K were observed in the photoluminescence (PL) of colloidal InP/ZnS core–shell nanocrystals. A subsequent study of PL spectra in the range 2–510 K and fitting the temperature dependent line shift and line width to theoretical models show that the dominant (dephasing) interaction is due to scattering by acoustic phonons of about 23 meV. Low temperature photoluminescence excitation measurements show that the excitonic band gap depends approximately inversely linearly on the quantum dot size *d*, which is distinctly weaker than the dependence predicted by current theories.

KEYWORDS: quantum dots · InP/ZnS · photoluminescence · temperature dependence · dephasing · size dependence · finite-size scaling

The synthesis of colloidal semiconductor nanocrystals (NCs) has seen an impressive progress in the past two decades, fueled by the unique physical properties of these nano-objects arising from quantum confinement. Among all II–VI and III–V semiconductor NCs, InP is probably the most promising compound, combining size-tunable emission in the visible and near-infrared spectral range (as the bulk band gap at room temperature is 1.35 eV[1]) and low intrinsic toxicity.[1−10] In view of the potential technological applications of semiconductor nanocrystals in biological labeling,[11] lasers,[12] LEDs,[13] and solar cells,[14] improvements in synthesis and structuring of these materials are still being made. Apart from the size-dependent properties, the band gap of semiconductor nanocrystals has been shown to depend on temperature[15−18] but the red shift of the emission upon raising the temperature is small and does not lead to clearly visible color changes.[19,20] In an earlier paper[21] we reported a study of the temperature dependence of both the band gap and photoluminescence (PL) line width in InP/ZnS nanocrystals in the temperature range 300–525 K. The results showed that, in this temperature range, the variation of *both* the energy band gap and the photoluminescence line broadening were predominantly due to coupling of the e_1-h_1 transition to acoustic phonons. We note that although the use of the term "band gap", by way of analogy with bulk semiconductors, has become common practice in the literature on quantum dots (QDs),[22,23] strictly speaking the quantity so denoted in QDs is the energy of the e_1-h_1 transition, commonly called the lowest exciton.

The variation of the band gap of semiconductors with temperature gives rise to color changes of emitted, transmitted, or reflected light. These color changes may have potential relevance in applications, as visual indicators for the temperature of a surface. By way of introduction to the paper, such distinct *visual* color changes in PL are reported here for semiconductor NCs, for the first time, to the best of our knowledge. The remainder of the paper is devoted to two issues directly related to these color changes. In the first part we investigate in detail the *temperature dependence* of both the PL peak energy and the PL line width over a wide temperature range (2–510 K) for QDs of various sizes (diameter 1.8–4.5 nm), and we analyze how this temperature dependence may be described and characterized by a few parameters. In the second part we investigate, at low temperature (2 K), the dependence of the PL peak energy and of the exciton energy upon the *size* of the QD, and we compare our results with recent theoretical predictions.

RESULTS AND DISCUSSION

Temperature Dependence in Photoluminescence. We start by considering the temperature dependence of the light emitted by the NCs in photoluminescence. Figure 1 shows for InP/ZnS core–shell nanocrystals of three different sizes, the

*Address correspondence to p.j.van.der.zaag@philips.com.

Received for review May 4, 2009 and accepted August 03, 2009.

Published online August 14, 2009.
10.1021/nn9004507 CCC: $40.75

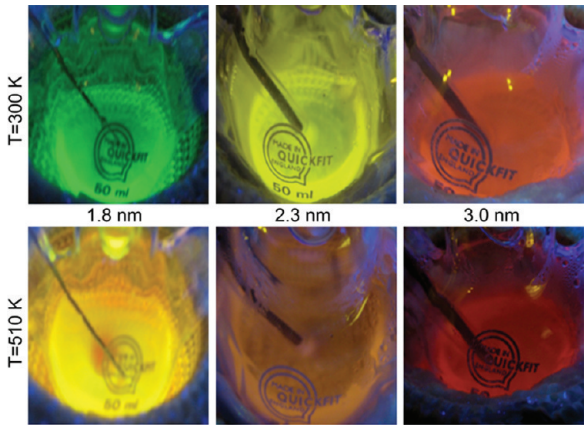

Figure 1. Photographs of solutions of InP/ZnS core−shell nanocrystals of three different sizes at room temperature (300 K) and 510 K, upon excitation with a Hg lamp.

color changes in the photoluminescence upon excitation by a Hg lamp when the temperature is raised from 300 to 510 K. The interesting aspect of this figure is that this is the first time such a distinct PL color change has been visually seen, whereas previously at most a change of shade had been observed.[18] The main reason why such prominent color changes were not observed in semiconductor nanocrystals in earlier reports[15−18] is that most temperature dependent studies are solely done in a cryostat up to 300 K (where visual inspection of the color is rarely done) and the fact that the color change is larger in the high temperature region (*vide infra*). Figure 2 shows the corresponding PL spectra at a number of different temperatures for a typical InP/ZnS core−shell nanocrystal sample.

We will first address the temperature dependence of the peak position of the PL spectra. Figure 3 shows the PL peak energy as a function of temperature for two samples of InP/ZnS core−shell NCs of different sizes (1.8 and 3.0 nm). The data in Figure 3 and of three more samples of differently sized InP/ZnS NCs could be fitted well to the Varshni expression,[24] which gives the temperature dependence of the band gap of bulk semiconductors and has also been used for quantum dots.[15,16,18,22]

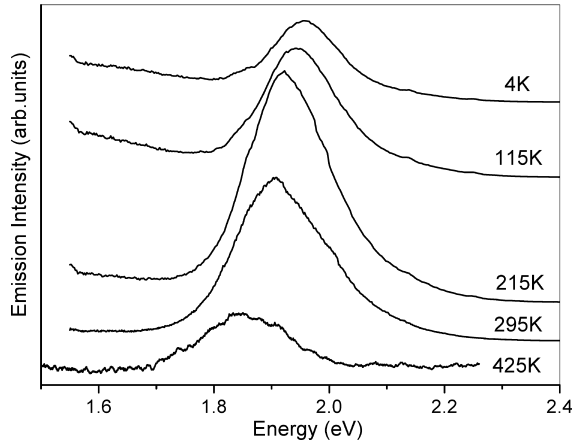

Figure 2. PL spectra of InP/ZnS core−shell quantum dot (3.8 nm) at five different temperatures.

$$E_g(T) = E_g(0) - \alpha T^2/(T + \beta) \quad (1)$$

where $E_g(0)$ is the bandgap at 0 K, α is the temperature coefficient, and the value of β is close to the Debye temperature. The Varshni expression should also be valid for the PL peak energy $E_{PL}(T)$ when the Stokes shift is independent of temperature, which we have verified to be the case for InP/ZnS quantum dots between 2 and 300 K. Note that, to distinguish the PL "band gap", that is, the PL peak energy shown in Figure 3, from the true excitonic band gap $E_g(T)$, we will henceforth refer to the PL peak energy as $E_{PL}(T)$. The results from the fits for InP/ZnS core−shell NCs of various sizes are tabulated in Table 1, where the values for $E_{PL}(0)$ are in fact the peak energies measured directly at 2 K, while those for α and β are obtained from the fit. Unlike the values of α, those of β agree with those reported for bulk InP ($\alpha = 4.91 \times 10^{-4}$ eV/K and $\beta = 327$ K).[24]

The theoretical basis for the much-used Varshni expression is unfortunately rather weak, as it is purely an empirical expression.[25] The parameter β, which is supposed to be of the order of the Debye temperature, in certain cases even turns out to be negative.[24] Moreover, eq 1 predicts a quadratic temperature dependence at low temperatures, whereas experimental results show (an approximate) temperature independence as can be seen from the insets in Figure 3. Hence, the data in Figure 3 were also fitted to a more recent expression proposed by O'Donnell and Chen,[26] which is expected to be an improvement over the Varshni expression, since it is based upon an analysis of the specific mechanism held responsible for the band gap narrowing, involving the electron−phonon coupling.

$$E_g(T) = E_g(0) - \frac{2S\langle\hbar\omega\rangle}{\exp(\langle\hbar\omega\rangle/k_BT) - 1} \quad (2)$$

where S is the Huang−Rhys factor, $\langle\hbar\omega\rangle$ is the average phonon energy, and k_B is the Boltzmann constant. The fitting results are tabulated in Table 2. The values of S from the fit signify that the electron−phonon coupling increases as the diameter of the nanocrystal is decreased. A similar trend was reported for CdSe quantum dots through fluorescence line narrowing.[27] Since a larger S results in a bigger band gap shift with temperature (see eq 2), the visual change in PL color is maximized by choosing smaller quantum dots as indicated by the data in Figures 1 and 3. This is in accordance with the theoretical analysis carried out by Schmitt-Rink and co-workers, who derived that $S \propto a_0^3/V$ where a_0 is the Bohr radius and V is the volume of the quantum dot.[28]

The average phonon energy obtained is much smaller than the longitudinal optical (LO) and transverse optical (TO) phonon energies of bulk InP,[29] yet is in accordance with the reported longitudinal acoustic

(LA) phonon energies (23.6 meV) derived from infrared spectroscopy and neutron scattering data for bulk InP.[30,31] The values in Table 2 are different from those reported in our previous study[21] (around 13 meV), which were similar to the value deduced from older Raman studies (15.5 meV).[32] The presently obtained values around 23 meV are considered to be more accurate since the full temperature range 2−510 K was included and $E_{PL}(0)$ was determined directly as opposed to being derived from the temperature fit, as was done in our earlier work.[21] It is interesting to note from Figure 3 that in the low temperature region (2−100 K) the Varshni expression gives a slightly better description of the data than eq 2. This indicates that a still better (physically relevant) model is required to give a good description of the observed shift at low temperatures.

Let us now turn our attention to the line width. Figure 4 shows the full width at half-maximum (fwhm) of the PL spectra as a function of temperature for the same two samples of InP/ZnS core/shell NCs for which the PL peak energies were shown in Figure 3. The data in Figure 4 can be fitted well to an expression which accounts for three contributions to the total line width,

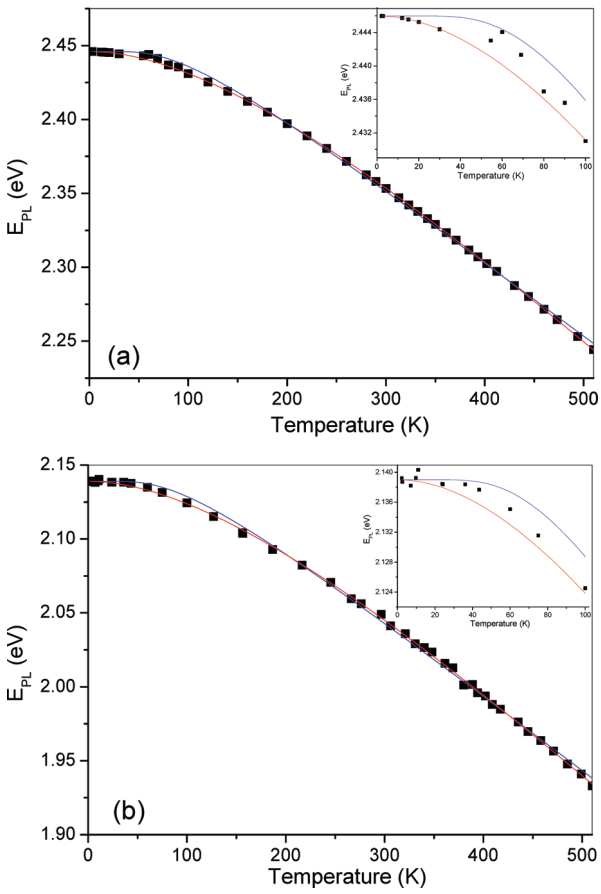

Figure 3. Photoluminescence peak energy as a function of temperature for InP/ZnS core/shell nanocrystals of (a) diameter = 1.8 nm and (b) diameter = 3 nm. Solid lines are the results of fitting the data to eq 1 (red) and eq 2 (blue) in the manuscript. The inset shows a magnified view of the data in the temperature range of 0−100 K.

TABLE 1. Parameters Used in the Fit of the PL Peak Energy as a Function of Temperature (Figure 3) by eq 1[a]

diameter *d* (nm)	$E_{PL}(0)$ (eV)	α (10^{-4} eV/K)	β (K)
1.8 ± 0.2	2.45 ± 0.01	6.5 ± 0.1	325 ± 10
2.1 ± 0.2	2.42 ± 0.01	6.3 ± 0.3	310 ± 30
3.0 ± 0.2	2.14 ± 0.01	6.7 ± 0.1	340 ± 15
3.8 ± 0.1	1.96 ± 0.02	4.5 ± 0.2	340 ± 30
4.5 ± 0.1	1.83 ± 0.02	3.5 ± 0.2	310 ± 40

[a]The zero-temperature peak energy $E_{PL}(0)$ was measured directly, whereas α and β were obtained from the fit.

viz., inhomogeneous broadening (due to fluctuations in size, shape, composition, *etc.* of the nanocrystals) and homogeneous broadening due to scattering of the exciton by optical phonons and by acoustic phonons, respectively.[16,33]

$$\Gamma(T) = \Gamma_{inh} + \sigma T + \Gamma_{LO}(\exp(E_{LO}/k_B T) - 1)^{-1} \quad (3)$$

where Γ_{inh} is the inhomogeneous line width, which is temperature independent, σ is the excitonic-acoustic phonon coupling coefficient, Γ_{LO} represents the strength of exciton−LO−phonon coupling and E_{LO} is the LO−phonon energy. The fitting results are tabulated in Table 3, where the values for Γ_{inh} are in fact measured directly at 2 K. While the values obtained for E_{LO} of about 40 meV are close to that for bulk InP, those obtained for σ and for Γ_{LO} are clearly different from the values for bulk InP (σ = 0.86 μeV/K, Γ_{LO} = 35.9 meV and E_{LO} = 42.8 meV).[33]

The slight reduction in the value of the optical phonon energy is consistent with the results obtained on CdSe/ZnS core−shell quantum dots, for which a reduction to 24.5 from 26.1 meV[34] (bulk value) has been reported.[16] Both optical and acoustic phonons are seen to contribute to the line broadening in InP/ZnS core−shell nanocrystals. At low temperatures the acoustic phonons contribution is dominant while the optical phonons only contribute at high temperatures. For instance, at 400 K the contribution to the total temperature-dependent line width from the acoustic phonons is ~85%. This can be seen clearly when only the acoustic contribution is plotted together with the constant inhomogeneous contribution, as shown in Figure 4 (red solid line).

Dot Size Dependence of Photoluminescence Peak Energy and Excitonic Band Gap. We now turn our attention to the effect of the size of the QDs on the optical properties. The sizes of the quantum dots were determined by low and high-resolution transmission electron microscopy (TEM). Representative TEM micrographs are shown in Figure 5 for three samples of InP/ZnS core−shell nanocrystals of different sizes. The NCs reveal themselves in the high-resolution images (right-hand side in Figure 5) as nearly spherical particles showing the cubic zinc

TABLE 2. Parameters Used in the Fit of the PL Peak Energy as a Function of Temperature (Figure 3) by eq 2[a]

diameter d (nm)	$E_{PL}(0)$ (eV)	S (Huang−Rhys factor)	$\langle\hbar\omega\rangle$ (meV) average phonon energy
1.8±0.2	2.45 ± 0.01	3.02± 0.02	23.1 ± 0.1
2.1±0.2	2.42 ± 0.01	2.45 ± 0.06	23.0 ± 0.2
3.0±0.2	2.14 ± 0.01	2.94 ± 0.03	23.3 ± 0.1
3.8±0.1	1.96 ± 0.02	1.93 ± 0.07	21.8 ± 0.5
4.5±0.1	1.83 ± 0.02	1.64 ± 0.03	22.8 ± 0.2

[a]The zero-temperature peak energy $E_{PL}(0)$ was measured directly, whereas S and $\langle\hbar\omega\rangle$ were obtained from the fit.

blende structure of InP. Determination of the diameter of the QDs was done manually from the images, with an estimated uncertainty between 0.1 and 0.2 nm, depending on QD size, comparable to widths of size distributions reported in the literature.[35] The diameter values thus determined include twice the thickness of the ZnS shell, which is calculated to be close to one monolayer, based upon the amount of shell precursors used.

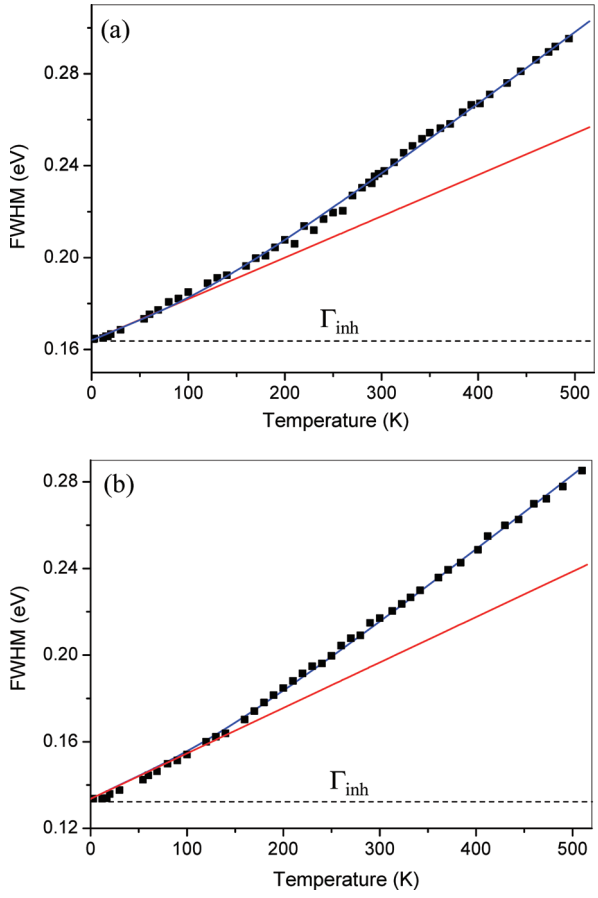

Figure 4. The fwhm of the peak observed in the PL spectra of InP/ZnS core−shell nanocrystals for two different sizes, as a function of temperature: (a) diameter = 1.8 nm and (b) diameter = 3.0 nm. Solid lines (blue) are the results of fitting the data to eq 3 in the manuscript. The contribution to the line width from the acoustic phonons along with the inhomogeneous broadening is shown as a red solid line, while the dotted line corresponds to the inhomogeneous broadening (Γ_{inh}).

TABLE 3. Parameters Obtained from the Fit of the fwhm of the PL Peak As a Function of Temperature (Figure 4) by eq 3[a]

diameter d (nm)	σ (μeV/K)	Γ_{LO} (meV)	E_{LO} (meV)	Γ_{inh} (meV)
1.8 ± 0.2	180 ± 8	68 ± 9	40 ± 5	164
2.1 ± 0.2	172 ± 6	60 ± 5	40 ± 5	154
3.0 ± 0.2	210 ± 7	63 ± 9	39 ± 6	134
3.8 ± 0.1	230 ± 6	56 ± 10	39 ± 5	103
4.5 ± 0.1	100 ± 4	32 ± 6	39 ± 6	95

[a]The inhomogeneous line width (Γ_{inh}) was measured directly while the other parameters were obtained from the fit.

Up to now most work on size dependence has relied on room temperature data, such as presented here for illustration in Figure 6, which shows room temperature emission spectra of our InP/ZnS nanocrystals of different sizes. However, since theoretical work generally gives zero-temperature energies, it is clearly preferable to make use of low temperature experimental data, such as presented in the section above. These results enable us to examine first of all, the dependence of the PL peak position on quantum dot size. Figure 7 shows this variation of the PL peak position (at 0 K) with respect to the diameter d of the InP/ZnS core−shell nanocrystals. Data from our previous study[21] have been included as well, and it is gratifying to note that those earlier PL peak positions obtained from temperature fits agree with the directly determined values from the present work. To analyze the corresponding size dependence the data in Figure 7 were fitted to the power law expression

$$E_{PL}(d) = E_{PL}(\infty) + A_{PL}/d^m \quad (4)$$

where $E_{PL}(d)$ is the PL peak energy of an InP quantum dot of size d at 0 K, $E_{PL}(\infty)$ is the PL peak energy of bulk InP at 0 K (1.375 eV[36]) and A_{PL} is a constant. The result of the fit is interesting: the shift of the peak position, $E_{PL}(d) - E_{PL}(\infty)$, is found to be close to inversely proportional to the QD size d (to be precise, the fit yields $m = 0.9 \pm 0.1$ and $A_{PL} = 1.9 \pm 0.2$ eV·nm). This is somewhat surprising as the closely related excitonic bandgap has been predicted to have a distinctly stronger size dependence, ranging for direct-band gap semiconductor QDs from $1/d^2$ according to effective mass theories[37,38] to $1/d^{1.36}$ according to pseudopotential calculations corrected for the electron−hole Coulomb energy specifically for InP by Fu and Zunger.[39]

As noted above, the PL peak energy in general contains a contribution from the Stokes shift and this complicates comparison with theoretical results. We therefore decided to measure on our samples the actual excitonic band gap by photoluminescence excitation spectroscopy (PLE), and, moreover, to do so at low temperature (actual measuring temperature ≅ 2 K). The latter aspect is important, because, as we have already seen above, E_g shows a significant temperature depen-

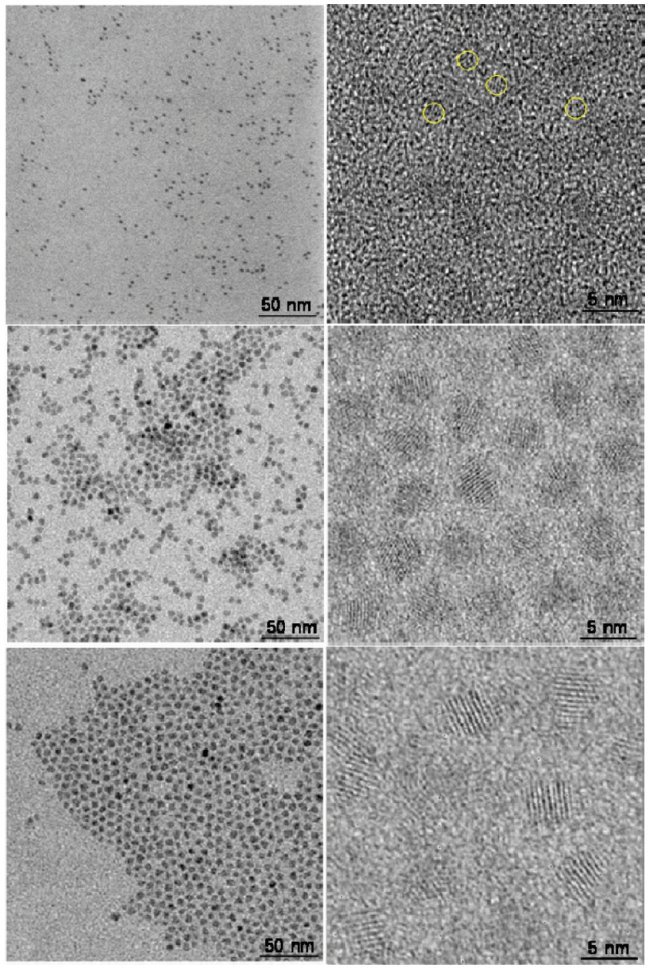

Figure 5. Low-resolution TEM images (on the left) and high-resolution TEM images (on the right) of three samples of InP/ZnS core−shell nanocrystals of different sizes: (from top to bottom) 1.8, 3.8, and 4.5 nm, respectively. In the HRTEM image of the 1.8 nm sample a few individual nanocrystals have been marked by yellow circles for clarity.

dence, so that only low temperature data (below 4 K) can provide a critical test of theoretical predictions, which are typically for 0 K.

Another nontrivial issue is what to take as the physically relevant size of the quantum dots. Two obvious alternatives present themselves. (A) The diameter of the entire InP/ZnS core−shell NCs as determined from TEM and used throughout above. This amounts to the rather extreme assumption that the ZnS shell does not produce any confinement of electron and/or hole, as if its electronic structure were identical to that of InP. (B) The diameter of the InP core as obtained by subtraction of twice the shell thickness, that is, $2 \times 0.35 = 0.70$ nm, from the TEM-determined value. This amounts to assuming infinitely strong confinement, which would seem more realistic because the InP/ZnS quantum dot electronic structure is type I and the bandgap of ZnS is considerably larger than that of InP (*viz.*, 3.84[40] *versus* 1.42 eV,[41] both at low T). Yet this assumption is also rather extreme, because the electron affinities of ZnS and InP do not differ much (3.9[40] and 4.4 eV,[41] respectively) so that the conduction band edges of ZnS and InP are quite close and consequently electrons are confined only weakly. Moreover, for such a thin shell it is not clear to what extent one can rely on considerations based upon bulk band structures. Therefore one had better consider these two alternatives as limiting cases, with the first one overestimating *d* and the second one underestimating *d*.

Thus we have plotted in Figure 8 the excitonic band gaps as measured by PLE *versus* the quantum dot diameter *d* according to alternative A (Figure 8a) as well as according to alternative B (Figure 8b). In each case they were fitted to the power law expression

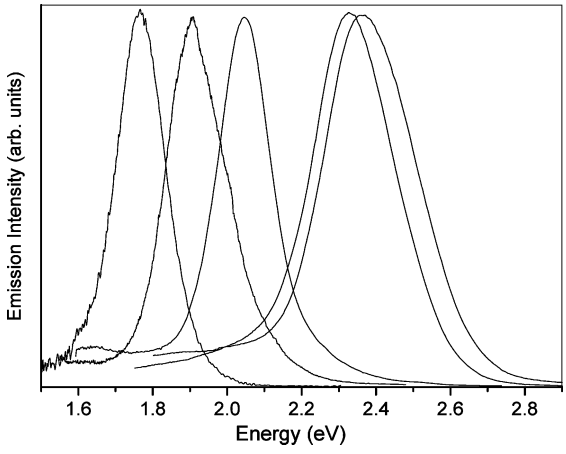

Figure 6. Room temperature PL spectra of InP/ZnS core−shell nanocrystals of five different sizes: (from left to right) 4.5, 3.8, 3.0, 2.1, and 1.8 nm, respectively.

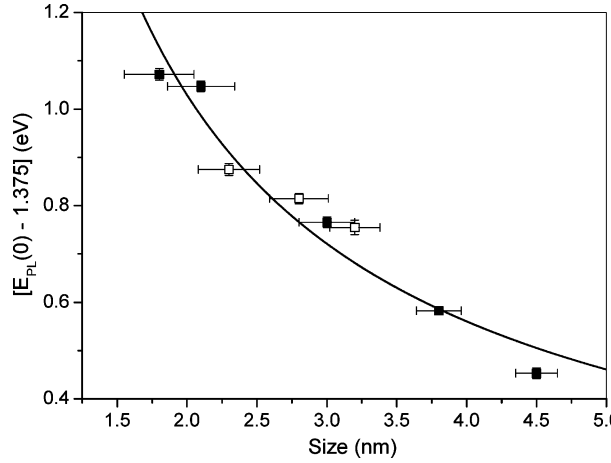

Figure 7. Photoluminescence peak energy at zero temperature as a function of the size of the InP/ZnS core−shell nanocrystals. Solid squares correspond to the data obtained in the present work, while open squares are taken from a previous study (ref 21). The solid line is the best fit to eq 4.

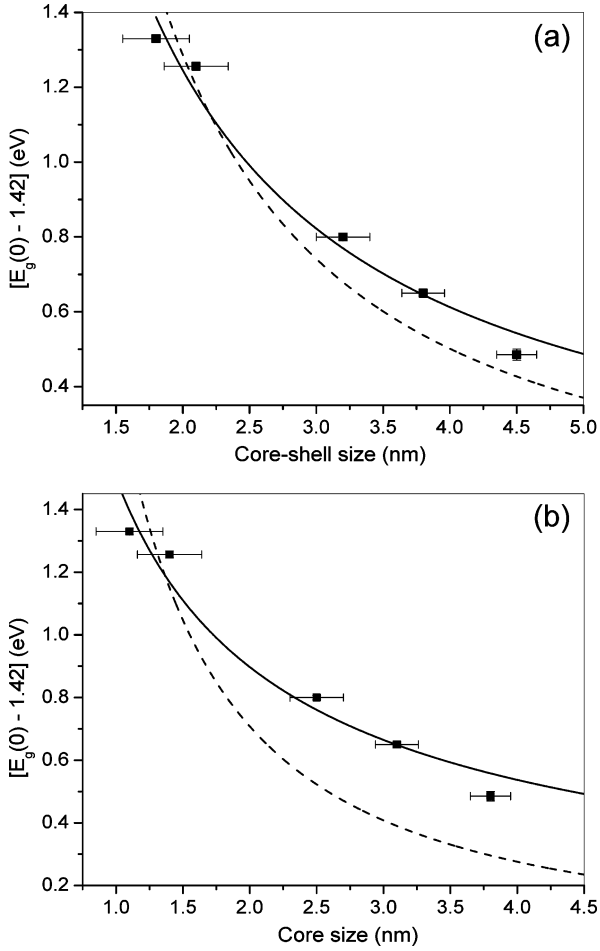

Figure 8. Excitonic band gap at zero temperature as a function of (a) the size of the InP/ZnS core−shell nanocrystals and (b) the size of InP cores. The solid lines are the best fits to eq 5 and the dotted lines are fits to eq 5 assuming a value of 1.36 for the exponent as calculated by Fu and Zunger (ref 39).

$$E_g(d) = E_g(\infty) + A_g/d^n \quad (5)$$

where $E_g(d)$ is the excitonic band gap at 0 K of quantum dots of size d, $E_g(\infty)$ is the excitonic band gap of bulk InP at 0 K (equal to 1.42 eV[41]) and A_g is a constant. The fits (solid lines in Figure 8) yield for alternative A (core−shell diameter) $A_g = 2.5 \pm 0.2$ eV · nm and a value for the exponent of $n = 1.03 \pm 0.09$ (the corresponding 95% confidence interval is [0.75, 1.29]), while for alternative B (core diameter) one finds $A_g = 1.5 \pm 0.1$ eV · nm and a value for the exponent of $n = 0.75 \pm 0.09$ (corresponding 95% confidence interval [0.48, 1.02]). For comparison we have also fitted the data to eq 5 with the exponent n fixed at the value 1.36 calculated by Fu and Zunger[39] (dashed lines in Figure 8). The poor quality of these fits clearly shows that this value of the exponent is not consistent with our 2 K data, which is further confirmed by the fact that it is outside the 95% confidence intervals. We note in passing that even the (room temperature) data of Mićić *et al.*,[2,42] from which Fu and Zunger concluded that $n = 1.36$ describes the size dependence rather well (see Figure 3 of ref 39), yield a value of 1.15 ± 0.1 for the exponent n when fitted directly to eq 5 if one uses the appropriate room temperature bulk value for $E_g(\infty)$ of 1.35 eV.[1] Thus we can firmly conclude that not only the PL peak energy but also the excitonic band gap shows a dependence on QD size that is quite close to inversely linear, and thus deviates significantly from the dependencies for direct band gap semiconductor QDs predicted by current theories[37−39,43] which characteristically give larger exponents.

CONCLUSIONS

The photoluminescence of InP/ZnS core−shell nanocrystals with various diameters has been investigated as a function of temperature in the temperature range 2−510 K. We find that the variation of both the PL peak energy and the PL line width is caused mainly by the coupling of the e_1-h_1 transition to the acoustic phonon modes. In the range 2−100 K the Varshni expression[24] describes the variation of the PL peak energy slightly better than the expression proposed by O'Donnell and Chen.[26]

The variation of the zero-temperature PL peak energy, and, more significantly, the variation of the zero-temperature excitonic band gap (as measured by PLE at 2 K) as a function of the size of the nanocrystals is found to be about inversely linear (*i.e.*, n is close to 1), rather than characterized by an exponent $n = 1.36$ as proposed by Fu and Zunger.[39]

METHODS

Materials. Indium acetate ($InAc_3$), myristic acid (MA), sulfur, 1-octylamine, and 1-octadecene (ODE) were purchased from Sigma Aldrich; zinc stearate was purchased from Alfa-Aesar; and tris(trimethylsilyl)phosphine ($P(TMS)_3$) was purchased from Strem chemicals.

Synthesis. In our previous study[21] InP nanocrystals were synthesized according to the procedure followed by Battaglia *et al.*[3] In the present work we have used the one-pot approach developed by Xie *et al.*,[6] because of the high quantum yields (30−40%) that can be obtained in comparison to the former. This helps to monitor the changes in the PL color with increasing temperature in a better way. In a typical synthesis of InP nanocrystals, 0.2 mmol of $InAc_3$, 0.77 mmol of MA and 4 g of 1-octadecene (ODE) were loaded into a three-necked flask. The mixture was heated to 188 °C under argon flow to obtain a clear solution. On reaching 188 °C a solution of $P(TMS)_3$ (0.1 mmol) and 1-octylamine (1.2 mmol) in ODE (0.75 mL in total) was injected rapidly. The injection brought down the temperature of the reaction to 175 °C for the growth of the nanocrystals. After 45 min, the temperature was lowered down to 150 °C.

The InP/ZnS core/shell synthesis was performed by the successive ion layer adsorption reaction (SILAR) method. The zinc injection solution (0.1 M) was prepared by dissolving zinc stearate in ODE at 140 °C. Similarly the sulfur injection solution (0.1 M) was prepared by dissolving sulfur in ODE at 120 °C. The zinc and sulfur precursor solutions (0.6 mL each) were injected sequentially into the reaction mixture at 150 °C. The waiting period be-

tween each injection was equal to 10 min. After that, the temperature was increased to 210 °C for 20 min to allow the growth of the ZnS shell. The InP/ZnS nanocrystals were purified from the reaction mixture by precipitation with acetone and redissolving them in toluene.

Photoluminescence of InP/ZnS core−shell nanocrystals in the temperature range 300−510 K was measured directly from the reaction flask using an Ocean Optics USB 2000 spectrophotometer. The temperature was determined using a thermocouple inserted directly into the reaction flask. For all nanocrystal sizes UV excitation was done using a Hg lamp, except for the 4.5 nm sized InP/ZnS nanocrystals where excitation was done by a Philips Lumiled Luxeon blue LED ($\lambda = 455$ nm). Low temperature (2−300 K) luminescence measurements were performed using an Edinburgh Instruments spectrofluorometer equipped with an Oxford Instruments Optistat CF flow cryostat. The solution of InP/ZnS quantum dots in toluene was cooled in a homemade quartz cuvette.

Transmission electron microscopy (TEM) was carried out using a TECNAI F30ST TEM operating at 300 kV. Samples for TEM studies were prepared by placing a 4 μL toluene solution of nanocrystals on ultrathin carbon-film-coated copper grids.

Acknowledgment. A.N. would like to acknowledge the financial support from the European Union Commission through a Marie-Curie fellowship. We thank M. A. Verheijen for performing TEM analysis, E. Verbitskiy for assistance with the statistical analysis, and P. van der Sluis for helpful discussions.

REFERENCES AND NOTES

1. Guzelian, A. A.; Katari, J. E. B.; Kadavanich, A. V.; Banin, U.; Hamad, K.; Juban, E.; Alivisatos, A. P.; Wolters, R. H.; Arnold, C. C.; Heath, J. R. Synthesis of Size-Selected, Surface-Passivated InP Nanocrystals. *J. Phys. Chem.* **1996**, *100*, 7212–7219.
2. Mićić, O. I.; Curtis, C. J.; Jones, K. M.; Sprague, J. R.; Nozik, A. J. Synthesis and Characterization of InP Quantum Dots. *J. Phys. Chem.* **1994**, *98*, 4966–4969.
3. Battaglia, D.; Peng, X. Formation of High Quality InP and InAs Nanocrystals in a Noncoordinating Solvent. *Nano Lett.* **2002**, *2*, 1027–1030.
4. Lucey, D. W.; MacRae, D. J.; Furis, M.; Sahoo, Y.; Cartwright, A. N.; Prasad, P. N. Monodispersed InP Quantum Dots Prepared by Colloidal Chemistry in a Noncoordinating Solvent. *Chem. Mater.* **2005**, *17*, 3754–3762.
5. Xu, S.; Kumar, S.; Nann, T. Rapid Synthesis of High-Quality InP Nanocrystals. *J. Am. Chem. Soc.* **2006**, *128*, 1054–1055.
6. Xie, R.; Battaglia, D.; Peng, X. Colloidal InP Nanocrystals as Efficient Emitters Covering Blue to Near-Infrared. *J. Am. Chem. Soc.* **2007**, *129*, 15432–15433.
7. Xu, S.; Ziegler, J.; Nann, T. Rapid Synthesis of Highly Luminescent InP and InP/ZnS Nanocrystals. *J. Mater. Chem.* **2008**, *18*, 2653–2656.
8. Li, L.; Reiss, P. One-Pot Synthesis of Highly Luminescent InP/ZnS Nanocrystals without Precursor Injection. *J. Am. Chem. Soc.* **2008**, *130*, 11588–11589.
9. Ryu, E.; Kim, S.; Jang, E.; Jun, S.; Jang, H.; Kim, B.; Kim, S.-W. Step-wise Synthesis of InP/ZnS Core−Shell Quantum Dots and the Role of Zinc Acetate. *Chem. Mater.* **2009**, *21*, 573–575.
10. Reiss, P.; Protiere, M.; Li, L. Core/Shell Semiconductor Nanocrystals. *Small* **2009**, *5*, 154–168.
11. Chan, W. C. W.; Nie, S. Quantum Dot Bioconjugates for Ultrasensitive Nonisotopic Detection. *Science* **1998**, *281*, 2016–2018.
12. Klimov, V. I.; Mikhailovsky, A. A.; Xu, S.; Malko, A.; Hollingsworth, J. A.; Leatherdale, C. A.; Eisler, H. J.; Bawendi, M. G. Optical Gain and Stimulated Emission in Nanocrystal Quantum Dots. *Science* **2000**, *290*, 314–317.
13. Colvin, V. L.; Schlamp, M. C.; Alivisatos, A. P. Light-Emitting Diodes Made from Cadmium Selenide Nanocrystals and a Semiconducting Polymer. *Nature* **1994**, *370*, 354–357.
14. Huynh, W. U.; Dittmer, J. J.; Alivisatos, A. P. Hybrid Nanorod−Polymer Solar Cells. *Science* **2002**, *295*, 2425–2427.
15. Suyver, J. F.; Wuister, S. F.; Kelly, J. J.; Meijerink, A. Luminescence of Nanocrystalline ZnSe:Mn^{2+}. *Phys. Chem. Chem. Phys.* **2000**, *2*, 5445–5448.
16. Valerini, D.; Creti, A.; Lomascolo, M.; Manna, L.; Cingolani, R.; Anni, M. Temperature Dependence of the Photoluminescence Properties of Colloidal CdSe/ZnS Core/Shell Quantum Dots Embedded in a Polystyrene Matrix. *Phys. Rev. B* **2005**, *71*, 235409/1–235409/6.
17. Al Salman, A.; Tortschanoff, A.; Mohamed, M. B.; Tonti, D.; Van Mourik, F.; Chergui, M. Temperature Effects on the Spectral Properties of Colloidal CdSe Nanodots, Nanorods, and Tetrapods. *Appl. Phys. Lett.* **2007**, *90*, 093104/1–093104/3.
18. Chin, P. T. K.; De Mello Donega, C.; Van Bavel, S. S.; Meskers, S. C. J.; Sommerdijk, N. A. J. M.; Janssen, R. A. J. Highly Luminescent CdTe/CdSe Colloidal Heteronanocrystals with Temperature-Dependent Emission Color. *J. Am. Chem. Soc.* **2007**, *129*, 14880–14886.
19. Liu, T.-C.; Huang, Z.-L.; Wang, H.-Q.; Wang, J.-H.; Li, X.-Q.; Zhao, Y.-D.; Luo, Q.-M. Temperature-Dependent Photoluminescence of Water-Soluble Quantum Dots for a Bioprobe. *Anal. Chim. Acta* **2006**, *559*, 120–123.
20. Liptay, T. J.; Ram, R. J. Temperature Dependence of the Exciton Transition in Semiconductor Quantum Dots. *Appl. Phys. Lett.* **2006**, *89*, 223132/1–223132/3.
21. Narayanaswamy, A.; Feiner, L. F.; Zaag van der, P. J. Temperature Dependence of the Photoluminescence of InP/ZnS Quantum Dots. *J. Phys. Chem. C* **2008**, *112*, 6775–6780.
22. Joshi, A.; Narsingi, K. Y.; Manasreh, M. O.; Davis, E. A.; Weaver, B. D. Temperature Dependence of the Band Gap of Colloidal CdSe/ZnS Core/Shell Nanocrystals Embedded into an Ultraviolet Curable Resin. *Appl. Phys. Lett.* **2006**, *89*, 131907/1–131907/3.
23. Dai, Q.; Song, Y.; Li, D.; Chen, H.; Kan, S.; Zou, B.; Wang, Y.; Deng, Y.; Hou, Y.; Yu, S.; *et al.* Temperature Dependence of Band Gap in CdSe Nanocrystals. *Chem. Phys. Lett.* **2007**, *439*, 65–68.
24. Varshni, Y. P. Temperature Dependence of the Energy Gap in Semiconductors. *Physica* **1967**, *34*, 149–154.
25. Thurmond, C. D. Standard Thermodynamic Functions for the Formation of Electrons and Holes in Germanium, Silicon, Gallium Arsenide, and Gallium Phosphide. *J. Electrochem. Soc.* **1975**, *122*, 1133–1141.
26. O'Donnell, K. P.; Chen, X. Temperature Dependence of Semiconductor Band Gaps. *Appl. Phys. Lett.* **1991**, *58*, 2924–2926.
27. Nirmal, M.; Norris, D. J.; Kuno, M.; Bawendi, M. G.; Efros, A. L.; Rosen, M. Observation of the "Dark Exciton" in CdSe Quantum Dots. *Phys. Rev. Lett.* **1995**, *75*, 3728–3731.
28. Schmitt-Rink, S.; Miller, D. A. B.; Chemla, D. S. Theory of the Linear and Nonlinear Optical Properties of Semiconductor Microcrystallites. *Phys. Rev. B* **1987**, *35*, 8113–8125.
29. Trommer, R.; Muller, H.; Cardona, M. Dependence of the Phonon Spectrum of InP on Hydrostatic Pressure. *Phys. Rev. B* **1980**, *21*, 4869–4878.
30. Borcherds, P. H.; Alfrey, G. F.; Saunderson, D. H.; Woods, A. D. B. Phonon Dispersion Curves in Indium Phosphide. *J. Phys. C* **1975**, *8*, 2022–2030.
31. Koteles, E. S.; Datars, W. R. Two-Phonon Absorption in Indium Phosphide and Gallium Phosphide. *Solid State Commun.* **1976**, *19*, 221–225.
32. Alfrey, G. F.; Borcherds, P. H. Phonon Frequencies from the Raman Spectrum of Indium Phosphide. *J. Phys. C* **1972**, *5*, L275–L278.
33. Rudin, S.; Reinecke, T. L.; Segall, B. Temperature-Dependent Exciton Linewidths in Semiconductors. *Phys. Rev. B* **1990**, *42*, 11218–11231.
34. Hellwege, K. H. *Numerical Data and Functional Relationship in Science and Technology*; Springer-Verlag: Berlin, 1982; Vol. *17*, Part B.
35. Mićić, O. I.; Jones, K. M.; Cahill, A.; Nozik, A. J. Optical, Electronic, and Structural Properties of Uncoupled and Close-Packed Arrays of InP Quantum Dots. *J. Phys. Chem. B* **1998**, *102*, 9791–9796.

36. Kang, J.; Matsumoto, F.; Fukuda, T. Photoluminescence of Undoped Bulk InP Grown by the Liquid-Encapsulated Vertical Bridgman Technique. *J. Appl. Phys.* **1997**, *81*, 905–909.
37. Ekimov, A. I.; Hache, F.; Schanne-Klein, M. C.; Ricard, D.; Flytzanis, C.; Kudryavtsev, I. A.; Yazeva, T. V.; Rodina, A. V.; Efros, A. L. Absorption and Intensity-Dependent Photoluminescence Measurements on Cadmium Selenide Quantum Dots: Assignment of the First Electronic Transitions. *J. Opt. Soc. Am. B* **1993**, *10*, 100–107.
38. Norris, D. J.; Bawendi, M. G. Measurement and Assignment of the Size-dependent Optical Spectrum in CdSe Quantum Dots. *Phys. Rev. B* **1996**, *53*, 16338–16346.
39. Fu, H.; Zunger, A. InP Quantum Dots: Electronic Structure, Surface Effects, and the Redshifted Emission. *Phys. Rev. B* **1997**, *56*, 1496–1508.
40. Madelung, O.; Rössler, U.; Schulz, M. *Landolt−Börnstein—Numerical Data and Functional Relationships in Science and Technology, New Series, Group III: Condensed Matter*; Springer-Verlag: Berlin, 1982; Vol. III/17b, 22a.
41. Vurgaftman, I.; Meyer, J. R.; Ram-Mohan, L. R. Band Parameters for III−V Compound Semiconductors and their Alloys. *J. Appl. Phys.* **2001**, *89*, 5815–5875.
42. Mićić, O. I.; Sprague, J.; Lu, Z.; Nozik, A. J. Highly Efficient Band-Edge Emission from InP Quantum Dots. *Appl. Phys. Lett.* **1996**, *68*, 3150–3152.
43. Lannoo, M.; Delerue, C.; Allan, G.; Niquet, Y. M. Confinement Effects and Tunneling Through Quantum Dots. *Phil. Trans. R. Soc. London, Ser. A* **2003**, *361*, 259–273.